CrystEngComm

Accepted Manuscript

ROYAL SOCIETY OF CHEMISTRY

www.rsc.org/crystengcomm

CrystEngComm

RSCPublishing

ARTICLE

Homogeneity limits and nonstoichiometry of vapor grown ZnTe and CdTe crystals

Cite this: DOI: 10.1039/x0xx00000x

I. Ch. Avetissov[a], E. N. Mozhevitina[a], A. V. Khomyakov[a], R. I. Avetisov[a], A. A. Davydov[b], V. P. Chegnov[b], O. I. Chegnova[b] and N. V. Zhavoronkov[b]

Received 00th January 2012,
Accepted 00th January 2012

DOI: 10.1039/x0xx00000x

www.rsc.org/

The homogeneity regions of zinc telluride ZnTe and cadmium telluride CdTe were studied by «the extraction» technique in 750-1365 K temperature range. It is shown that the homogeneity region of undoped ZnTe contains stoichiometric composition. The existence of wurtzite-based ZnTe at high temperatures was proved and its lattice parameters were determined. A scheme of 3C-2H polymorphous transition for ZnTe compounds is proposed in which the transition is followed by peritectic reactions at both Te-rich and Zn-rich sides. In the case of CdTe the solidus line near the melting point demonstrated anomalous behavior which could be explained in terms of high-temperature polymorphous transition but the polymorph was not fixed due to the low transition energy. The undoped ZnTe and CdTe single crystals were obtained by the Markov-Davydov vapor growth technique under pressures close to congruent sublimation conditions in the temperature range 1170-1320 K. Nonstoichiometry and impurity distribution in 60 mm diameter ZnTe and 100 mm diameter CdTe vapor grown crystals were examined.

Introduction

Cadmium telluride (CdTe) and its alloys (Cd,Zn)Te are basic materials for gamma-detectors of new generation operating at room temperature [1]. ZnTe single crystals are widely use as IR optical applications, substrates for green LEDs and LDs [2,3]. However, crystal growth of these materials, especially with large diameters, encounters some serious problems [4]. In general, crystal growth from melt engages the solidus line as a starting point of crystallization process. Apart from very low thermal conductivity, probable high temperature polymorphs and structure reconstruction during cooling may cause problems in the CdTe and ZnTe melt crystal growth.

It is known that there are two stable polymorphs at the normal pressure in ZnS, ZnSe, CdS, CdSe semiconductors: the high temperature wurtzite, and the low temperature sphalerite [5]. Nevertheless, there are no available data concerning existence of a wurtzite-based phase in bulk CdTe or ZnTe. Single crystals based on CdTe and ZnTe used in multipurpose devices are required to have a pure sphalerite structure.

The problem of polymorphous transition at a crystal cooling can be avoided by growing these crystals by the THM [6] or vapor [7] techniques. Still, the THM technique has encountered the same fundamental problems, as the conventional Bridgman technique, namely, the melt capture and large concentrations of nonstoichiometry defects according to the solidus lines. The vapor growth allows direct obtainment of a low-temperature sphalerite phase of an as-grown single crystal. On the other hand, low growth rates and a difficulty of production of large diameter crystals are disadvantages of vapor growth techniques.

In the present research, we investigate the problem of ZnTe and CdTe non-stoichiometry with the emphasis on homogeneity regions and analyse non-stoichiometry of ZnTe and CdTe vapor grown crystals by a direct physicochemical method.

Study of nonstoichiometry

In this study, we paid particular attention to purity at all steps of the experimental procedure. The initial powdered CdTe and ZnTe (ELMA, Russia, nominally 99.999 wt%) were additionally refined by re-sublimation under high vacuum. Analyses of the final purity (including O, C, N, F, Cl) determined by ICP-MS (NexION 300D, Perkin Elmer Inc.) and SIMS (MiniSIMS, Millbrook Ltd.) delivered 99.99989 and 99.99968 wt% for CdTe and ZnTe, correspondingly. High temperature annealing was conducted in the 720-1369 K temperature range in extra-pure quartz glass ampoules with inner pyrocarbon coating evacuated to 10^{-5} Torr.

Method of nonstoichiometry determination

CdTe and ZnTe homogeneity regions were examined by high-temperature equilibrium $S_{ZnTe(CdTe)}LV$ freezing technique [8]. Deviations from stoichiometric compositions of quenched samples were determined using the "extraction" (direct

physico-chemical) method [9] based on the evaporation of an excess component of analyzed preparation at controlled temperature ($T_{exctraction}$) from the "hot" zone of the evacuated ampoule (Fig.1a), a vapor violation to the "cold" zone of the ampoule, and a vapor condensation on the ampoule walls at $T_{condensation} < T_{extraction}$. The quantitative analysis of a condense phase of an excess component was made by ICP-MS.

In general, congruent sublimated composition does not match to stoichiometric composition. The main idea of the developed «extraction» technique is to find out the conditions when these two compositions differ less than the determination accuracy. Fig.1b,c shows what part of an excess component one could extract in the process at various $T_{extraction}$ (T_1 or T_2) and $P_{A\text{-}excess}$ ($T_{condensation}$) from nonstoichiometric AB preparation, which contains 1×10^{-3} excess of A component (red point on Fig.1b). The lowest $P_{A\text{-}excess}$ at the certain $T_{extraction}$ is determined by congruent sublimation conditions (S_{AB}=V).

At T_1 under S_{AB}=V conditions one gets a preparation with 1×10^{-3} excess of B component in nonstoichiometric AB. It means that during the extraction process at T_1 one extracts 1×10^{-3} excess of A component until δ=0 and another 8×10^{-4} (see Fig 1c) of A component until one reaches the equilibrium state of the system at S_{AB}=V. Totally, one extract 1.8×10^{-3} of A component. It will be nearly in 2 times more than the preparation nonstoichiometry (1×10^{-3} excess of A component).

At T_2 under S_{AB}=V conditions one obtains a preparation with 1×10^{-5} excess of B component in nonstoichiometric AB and during the extraction one extracts 1×10^{-3} excess of A component until δ=0 and another 1×10^{-5} (see Fig 1c) of A component until the equilibrium state of the system at S_{AB}=V will be reached. The real accuracy of chemical analysis is 2÷8 rel. % for 10^{-6} g amounts of determined components (see Tables 1,2). It means that 1×10^{-5} over-extracted A component will be less than the determination error.

We should find the extraction conditions which provided a residual nonstoichiometric composition of the sample to be at least one order lower (10 rel. %) in comparison with the determined value of nonstoichiometry - X_A^{excess} (relative quantity of extracted excess component A – ΔX_A). In this case we could assert $X_A^{excess} = \Delta X_A$. To find the certain «extraction» regime for the certain $A^{II}B^{VI}$ substance we studied the «extraction» process kinetics depending on powdered preparation's size (15÷500 μm) as well as temperature regimes for both $T_{extraction}$(700÷1100 K) and $T_{condensation}$(560÷950 K). We also proved the final equilibrium state by its reversibility. Finally, we got the regimes with a declared accuracy of nonstoichiometry determination. In the cases of ZnTe and CdTe we measured the nonstoichiometry with the accuracy ±(2÷7) rel.% in the range 10^{-4}÷5×10^{-8} mole excess Te(Cd,Zn)/ mole ZnTe (CdTe).

Application of the "extraction" technique to nonstoichiometry investigations puts negligible restrictions on quenching quality. There is no need to keep a high-temperature state of native point defects. It is enough that an excess component has not left the solid while quenching.

The quenching efficiency was examined by varying the polycrystalline powder average size (from 20 to 500 μm) and ampoule freezing conditions (open air or water with ice). In 750-1365 K temperature range reproducible results within ±18 percent were obtained for the preparations quenched in water with ice not depending on a powder size.

ZnTe homogeneity limits

For the first time we found Zn-solubility in ZnTe. Limits of Zn-solubility in ZnTe crystals were examined in the 765-1356 K temperature range (Table 1). The Zn-solubility and also the solidus line proved to be retrograde (Fig.1).

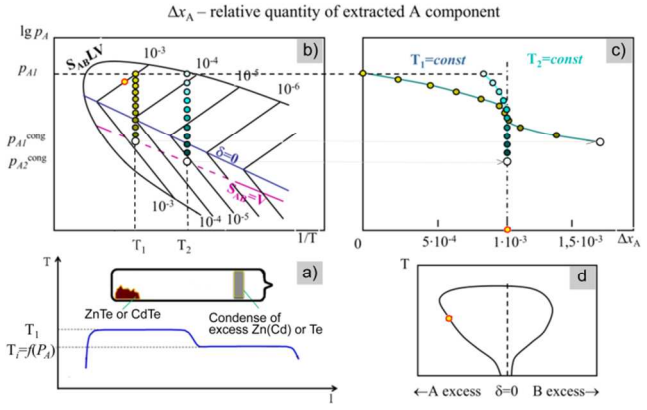

Fig. 1 The scheme of «extraction» technique for determination of nonstoichiometry in case of congruent sublimating (S_{AB}=V) AB binary compound with double side homogeneity range: • - the search nonstoichiometry, the lowest P_A at T_i is determined by S_{AB}=V conditions, at T_1 one extracts more A component than in the search nonstoichiometry, at T_2 the largest extracted A component corresponds to the search nonstoichiometry while the residual nonstoichiometry (10^{-5}) is in two orders less than the search one

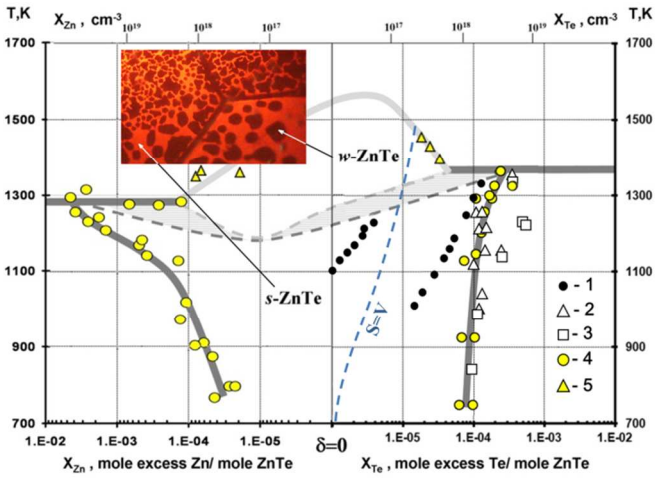

Fig. 2 Homogeneity region of ZnTe with the assumed scheme of 3C-2H polymorphous transformation: 1- ionized defects calculated by [10], 2-[11], 3-[12], 4, 5-our data. In case of Δ points we observed traces of *w*-ZnTe on XRD patterns of quenched samples and anisotropic parts (dark) on micrographs in polarized light (see insertion) contrary to isotropic *s*-ZnTe (light).

For the Te-rich side in 750-1455 K temperature range we obtained the retrograde solidus, while the Te-limits were by a half smaller than those earlier published [11]. The determined Te-nonstoichiometry exceeded the nonstoichiometry calculated from ionized defect concentrations [10] at the temperatures below 1300 K. This allows the assumption that dominant native point defects at the Te-rich side at low temperatures could be electrically neutral.

Table 1 Deviation from stoichiometry in ZnTe preparations at monovariant equilibria

Synthesis			Analysis		$X_{Te(Zn)}^{excess}$,
T, K	Time, hour	m_{ZnTe}, g	$m_{Zn}\times10^6$, g	$m_{Te}\times10^6$, g	mole excess Te (Zn)/ mole ZnTe
			$S_{ZnTe}L_{(Te)}V$		
750	208	0.5648	13.1±1.2	61.6±8	$(9.65\pm2.80)\times10^{-5}$
750	208	0.8105	2.5±0.1	38±4	$(6.18\pm0.75)\times10^{-5}$
925	120	1.5556	3.7±0.2	111.8±12	$(1.02\pm0.12)\times10^{-4}$
925	120	1.4406	0±0	64.3±6.3	$(6.75\pm0.65)\times10^{-5}$
1128	105	0.9614	0±0	46.1±6.1	$(7.25\pm0.93)\times10^{-5}$
1146	105	1.0526	4±0	82.1±7.0	$(1.07\pm1.03)\times10^{-4}$
1201	72	1.1023	4±0	100±11	$(1.26\pm0.15)\times10^{-4}$
1256	72	2.0844	2±0	195±18	$(1.39\pm0.13)\times10^{-4}$
1291	65	2.7432	0±0	322±26	$(1.78\pm0.14)\times10^{-4}$
1291	65	1.3759	3.3±0.1	102.8±5.2	$(1.06\pm0.06)\times10^{-4}$
1300	54	0.9963	0±0	107±3.1	$(1.62\pm0.05)\times10^{-4}$
1325	54	2.6636	0±0	341±10	$(1.94\pm0.06)\times10^{-4}$
1325	54	1.5049	0±0	340±10	$(3.42\pm0.10)\times10^{-4}$
1363	48	1.8912	0±0	291±40	$(2.33\pm0.32)\times10^{-4}$
1397	50	0.8093	3.5±0.3	24.6±1.5	$(3.32\pm0.28)\times10^{-5}$
1430	50	1.0848	0.9±0.1	19.3±4.3	$(2.45\pm0.60)\times10^{-5}$
1455	50	1.0879	5.9±0.2	24.9±2.8	$(1.86\pm0.39)\times10^{-5}$
			$S_{ZnTe}L_{(Zn)}V$		
765	282	0.8901	17.0±5.0	8±4	$-(4.28\pm2.34)\times10^{-5}$
795	282	1.6156	14.5±2.6	0±0	$-(2.65\pm0.48)\times10^{-5}$
795	282	2.4105	18.0±2.1	0±0	$-(2.20\pm0.26)\times10^{-5}$
873	201	2.1254	35.7±5.1	4.9±0	$-(4.61\pm0.74)\times10^{-5}$
902	201	1.2654	34.7±2.2	0±0	$-(8.09\pm0.51)\times10^{-5}$
909	201	0.9017	23.7±6.1	10.3±1.1	$-(6.03\pm0.21)\times10^{-5}$
1016	150	1.0045	36.5±0.9	0±0	$-(1.01\pm0.03)\times10^{-4}$
1126	150	0.5736	26.8±0.6	0±0	$-(1.38\pm0.03)\times10^{-4}$
1140	124	1.0716	172±10	64.6±3.0	$-(3.82\pm0.32)\times10^{-4}$
1168	124	0.7860	128±2.5	0±0	$-(4.79\pm0.09)\times10^{-4}$
1181	124	1.0926	209±8.0	87.8±2.0	$-(4.42\pm0.24)\times10^{-4}$
1205	72	1.0009	475±3.7	0±0	$-(1.40\pm0.11)\times10^{-3}$
1228	72	0.6681	560±8.4	0±0	$-(2.47\pm0.04)\times10^{-3}$
1241	71	0.9781	581±21	0±0	$-(1.75\pm0.06)\times10^{-3}$
1254	71	0.9967	1270±10	0±0	$-(3.75\pm0.02)\times10^{-3}$
1292	64	1.0448	1560±20	0±0	$-(4.41\pm0.06)\times10^{-3}$
1275	64	1.0197	229±7.9	0±0	$-(6.63\pm0.23)\times10^{-4}$
1271	64	1.0393	91.8±19	0±0	$-(2.61\pm0.54)\times10^{-4}$
1280	68	0.9921	80.0±12	75.0±8.1	$-(1.24\pm0.48)\times10^{-4}$
1313	60	1.0305	916±15	0±0	$-(2.62\pm0.06)\times10^{-3}$
1347	60	1.8653	50.6±3.3	2.9±0.2	$-(7.77\pm0.52)\times10^{-5}$
1356	45	1.9307	13.6±5.0	2.3±0.2	$-(1.90\pm0.76)\times10^{-5}$

"–" indicates on Zn excess in ZnTe preparations.

We made the optical microscopy analysis of a boule (~1 mm) which had been recrystallizing and growing up during annealing under condition close to $S_{ZnTe}L_{(Te)}V$ equilibrium and quenched from T>1365 K. The boule had X_{Te}^{excess}= $(1.8\div3.3)\times10^{-5}$ mole excess Te/ mole ZnTe. We observed areas of two types (Fig. 2 insertion): a transparent orange area (I type) with distinct block boundaries and opaque dark-red droplets (II type). According to ICP-MS and SIMS the boule purity was of 99.9996 wt%, hence, the observed droplets could not be attributed to impurities. Their existence could be explained in terms of two phases with different crystal structures.

A polarized microscopy testing showed that the I-type phase did not demonstrate birefringence – it was optically isotropic and we consider it to be cubic sphalerite ZnTe (*s*-ZnTe). The II-type phase occurred to be optically anisotropic and periodically dimming while rotating at crossed nicols, and we attributed it to the wurtzite ZnTe (*w*-ZnTe) appearing to be not less 30 vol. % of the sample. XRD analysis of powdered samples proved the presence of hexagonal *w*-ZnTe (Fig. 3). So, for the first time, evidence was achieved for a hexagonal *w*-ZnTe existence in a bulk crystal at high temperatures and normal pressures.

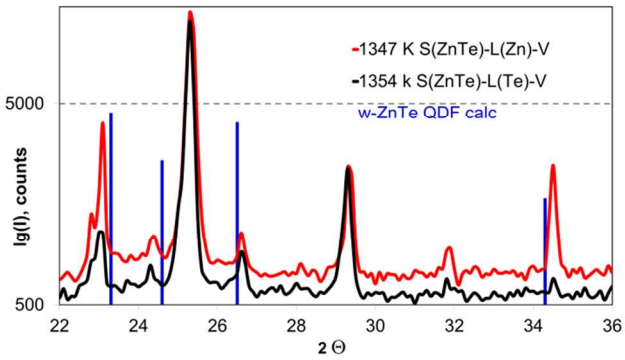

Fig. 3 XRD patterns of powdered ZnTe samples with wurtzite phase traces quenched from 1347 K (red line) and 1354 K (black line) after annealing under $S_{ZnTe}L_{(Zn)}V$ equilibrium

Up to now, the ZnTe wurtzite structure was found in thin films [13] or as a result of simulation of wurtzite ZnTe structure [14]. Considering a finite quenching rate and a low energy of wurtzite- sphalerite phase transition (for ZnS $\Delta H_{w\text{-}s}$= 0.29 KJ/mole [15] and for CdSe $\Delta H_{w\text{-}s}\cong$ 0.48 KJ/mole [16]), we assumed that traces of *w*-ZnTe phase in quenched samples denoted the existence of the equilibrium *w*-ZnTe phase at high temperatures. For the lattice parameters of *w*-ZnTe we found out a=0.436±0.002 nm, c=0.7144±0.0002 nm, c/a=1.638. The last value coincides with that ones for *w*-ZnS and *w*-ZnSe [17]. We also found traces of wurtzite ZnTe (*w*-ZnTe) in the samples synthesized under $S_{ZnTe}L_{(Zn)}V$ equilibrium at T>1290 K and $S_{ZnTe}L_{(Te)}V$ equilibrium at T>1350 K.

Taking into account XRD data and possible schemes of polymorphous transition we represent the ZnTe homogeneity range with the proposed wurtzite-sphalerite (3C-2H) transition (Fig. 2). In the preparations marked as triangles we observed the traces of *w*-ZnTe phase. According to the scheme 3C-2H polymorphous transition is accompanied by peritectic reactions from both the Te-rich and Zn-rich sides.

CdTe homogeneity limits

The CdTe homogeneity range was studied in the 970-1365 K temperature range (Table 2). At temperatures close to CdTe

T_m^{max} we observed a strong retrograde behavior of the solidus (Fig. 4). A similar pattern was presented by Ivanov [20], who used extra-pure source materials and a direct extraction technique for non-stoichiometry measurements.

Table 2 Deviation from stoichiometry in CdTe preparations at monovariant equilibria

Synthesis			Analysis		$X_{Cd(Te)}^{excess}$,
T, K	Time, hour	m_{CdTe}, g	$m_{Cd}\times10^6$, g	$m_{Te}\times10^6$, g	mole excess Cd (-Te)/ mole CdTe
			$S_{CdTe}L_{(Cd)}V$		
882	360	0.8631	13.6±0.1	0.38±0.03	(5.70±0.35)×10^{-5}
1022	320	1.2799	22.3±1.1	4.36±0.78	(5.75±0.35)×10^{-5}
1071	208	0.7258	102±8	5.3±0.5	(4.41±0.35)×10^{-5}
1122	208	1.2949	26.9±1.3	2.63±0.10	(7.23±0.35)×10^{-5}
1196	208	1.5846	66±5	0.0±0.0	(1.46±0.12)×10^{-4}
1207	120	2.1160	84±9	15±1	(7.13±0.89)×10^{-5}
1268	120	1.9853	172±14	10±1	(7.85±0.63)×10^{-4}
1270	105	1.9826	715±16	219±1	(5.61±0.18)×10^{-4}
1271	105	1.5331	78±3	7.0±1.0	(9.99±0.41)×10^{-5}
1279	72	0.9925	255±4	29±2	(4.94±0.12)×10^{-4}
1289	72	1.2660	530±70	21±4	(8.62±1.10)×10^{-4}
1323	65	0.9707	553±28	75±6	(1.07±0.11)×10^{-3}
1348	65	0.8726	156±7	31±1	(3.15±0.13)×10^{-4}
1345	54	1.2159	88±7	0.0±0.0	(1.54±0.12)×10^{-4}
1345	54	1.1443	123±10	0.0±0.0	(2.31±0.19)×10^{-4}
1345	54	1.4011	341±14	0.0±0.0	(5.19±0.21)×10^{-4}
1354	48	1.0010	82±6	7.0±0.0	(1.62±0.12)×10^{-4}
			$S_{CdTe}L_{(Te)}V$		
943	282	1.8543	11±1	156±10	-(4.28±2.34)×10^{-5}
1053	282	1.1226	15±4	170±10	-(2.65±0.48)×10^{-5}
1100	282	1.1562	18±2	406±33	-(2.20±0.26)×10^{-5}
1175	201	1.4512	100±17	139±10	-(4.61±0.74)×10^{-5}
1207	201	2.5902	21±2	10300±75	-(8.09±0.51)×10^{-5}
1271	201	1.3876	26±3	926±23	-(6.03±0.21)×10^{-5}
1289	150	1.3856	138±19	8255±190	-(1.01±0.03)×10^{-4}
1323	150	1.1265	21±4	338±15	-(1.38±0.03)×10^{-4}
1348	124	0.5157	88±7	0±0	-(3.82±0.32)×10^{-4}

"–" indicates on Te excess in CdTe preparations.

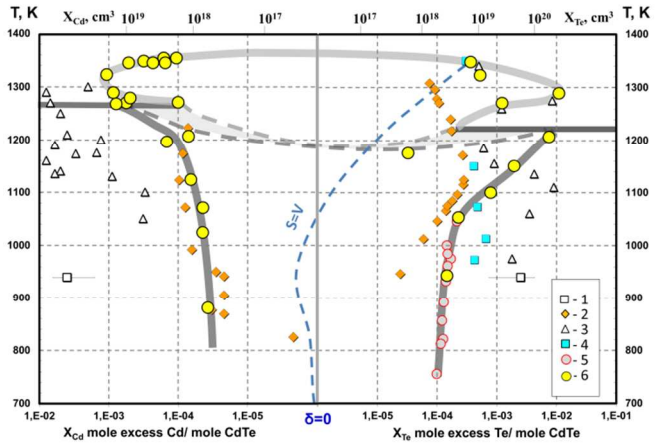

Fig. 4 Homogeneity region of CdTe with the supposed scheme of high temperature polymorphous transformation: 1-[18], 2-[19], 3-[20], 4-[21], 5-[22], 6- our data

At lower temperatures we also obtained the retrograde solidus for both the Cd-rich and Te-rich sides. For the Cd-rich side at T<1200 K and the Te-rich side at T<1050 K our data were close to those [19,22] obtained by the Burdone manometer technique. The existence of high-temperature polymorphous transformation in CdTe was proved experimentally by p_t–T–x diagram analysis [26]. A high temperature polymorph was supposed to have wurtzite structure – (*w*)-CdTe [4,26].

The thermodynamic estimation of enthalpy of the 3C-2H polymorphous transition in CdTe [27] gave the value $\Delta H_{(w)\text{-CdTe}\rightarrow s\text{-CdTe}} = -120$ J/mole CdTe at ~1270 K, which is too low for a successful quenching of the assumed high-temperature *(w)*-CdTe polymorph. Considering these data and the determined behavior of the solidus line we suppose a scheme of 3C-2H polymorphous transition in CdTe, which is similar to that of ZnTe. We suppose that in both cases the polymorphous transitions are followed by peritectic reactions at both the Te-rich and Cd-rich sides (Fig.4).

General schemes of dominant point defect generation in CdTe and ZnTe

There are a large variety of native point defects assumed to present in *s*-CdTe [4]. At $S_{CdTe}LV$ equilibrium they are mostly electrically neutral [4,23], while in the case of ZnTe for the Te-rich side electrically active defects contribute significantly in total nonstoichiometry in 1100-1300 K temperature range (see Fig.2). But till now nobody has detected *n*-type conductivity in undoped ZnTe attributed to native donor point defects. There is a need in Te vacancies to explain oxidation processes in ZnTe [28]. On the other hand there are a numerous facts proved a high disordering in CdTe at temperatures close to T_m^{max}[4]. And we also got a small slope for dependence of $x_{Zn}^{excess} = f(p_{Zn})$ at T=1250 K under bivariant $S_{s\text{-ZnTe}}V$ equilibrium (Fig.5).

Taking into consideration a similarity of ZnTe and CdTe properties to describe the experimental data we expected the following types of native point defects presented in Table 3. A special attention should be paid on a complex defect $(Me_i(V_{Me}^{\times})_4)^{\times}$, which is responsible for a strong disordering and possibility to generate microprecipitates at a crystal cooling. The latters are typical defects in CdTe single crystals grown under higher Cd partial pressure [4].

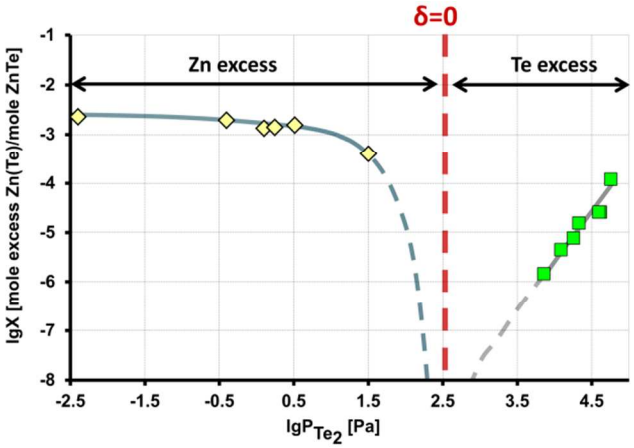

Fig. 5 Nonstoichiometry of ZnTe at $S_{ZnTe}V$ equilibrium at 1250 K

To avoid microprecipitation somebody used special cooling regimes [29]. Another way to get precipitate free CdTe crystals consists in their growth from vapor under bivariant $S_{AB}V$ conditions inside the homogeneity region [4].

Growth technique and crystal characterization

ZnTe and CdTe single crystals were grown from vapor the by the Markov-Davydov technique [7] (Fig. 6) without contact of a growing crystal with reactor walls (4) by sublimation of a polycrystalline ingot (5) from a crucible (6) towards a seed (8) placed on a sapphire pedestal (9), while a part of the source material was slipping into the low-temperature zone of the reactor (10) below the pedestal.

.

Table 3 The reactions of dominant native point defects generation in *s*-ZnTe and *s*-CdTe at $S_{AB}LV$ equilibria. $K=K_0\exp(-\Delta H_r/RT)$

Reaction	Constant of the reaction	K_0		ΔH_r, kJole/mole	
		ZnTe	CdTe	ZnTe	CdTe
Metal disordering					
$Me^v \rightarrow Me_{Me}^{\times} + V_{Te}^{\times}$	$K = [V_{Te}^{\times}]/p_{Me}$	4.17×10^{-13}	4.35×10^{-14}	-81.035	-80.6
$Me^v \rightarrow Me_i^{\times} + V_{Te}^{\times}$	$K = [Me_i^{\times}]\cdot[V_{Te}^{\times}]/p_{Me}$	4.99×10^{-8}	1.40×10^{-7}	9.065	43.4
$Me^v \rightarrow (Me_i(V_{Me}^{\times})_4)^{\times} + 4V_{Te}^{\times}$	$K = [(Me_i(V_{Me}^{\times})_4)^{\times}]\cdot[V_{Te}^{\times}]^4/p_{Me}$	8.49×10^{7}	4.70×10^{12}	279.365	415.4
Chalcogen disordering					
$Te_2{}^v \rightarrow Te_{Te}^{\times} + (V_{Me}^{\times})_2$	$K = [(V_{Me}^{\times})_2]/p_{Te2}$	5.30×10^{-15}	4.27×10^{-6}	-116.4	-17.1
$1/2\,Te_2{}^v \rightarrow Te_{Te}^{\times} + V_{Me}^{\times}$	$K = [V_{Me}^{\times}]/p_{Te2}^{1/2}$	1.69×10^{-10}	4.18×10^{9}	-63.6	277.8
$1/2Te_2{}^v \rightarrow Te_{Te}^{\times} + V_{Me}'' + 2h^{\cdot}$	$K = [V_{Me}'']\cdot p^2/p_{Te2}^{1/2}$	1.14×10^{-24}		48.397	

Crystals were formed at 1170-1320 K temperature range at a pressure remaining close to congruent sublimation conditions (dash blue line on Fig. 2 and Fig. 4).

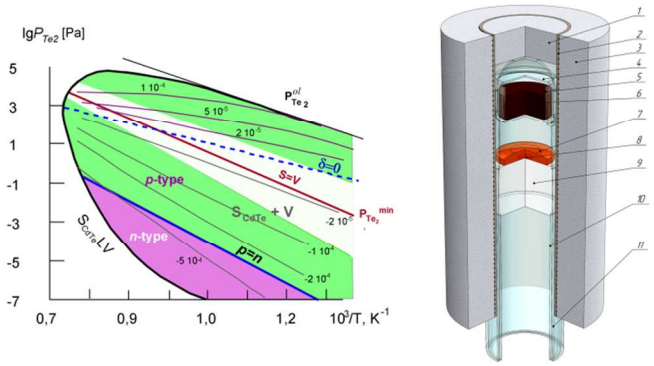

Fig. 6 Scheme of crystal growth from vapor by Markov-Davydov technique [7]. Growth setup configuration (right): 1- thermo insulating cover, 2 – ceramic tube, 3-thermoinsulation, 4 – quartz glass reactor, 5- polycrystalline ingot, 6- quartz glass crucible, 7- growing crystal, 8- seed, 9- polished sapphire pedestal, 10- quartz glass tube, 11- outlet for vacuum system connection. P_{Te2}-T projection of *s*-CdTe (left) [23-25]: figures on lines show the constant excess Te («-» Cd), concentrations, at $S_{s\text{-}CdTe}V$ bivariant equilibrium. The white color area indicates the parameter range for a stable single crystal vapor growth

The growth proceeded with 0.05-0.1 mm/h growth rate due to the low thermal conductivity and insufficient heat removing at fast crystallization. The growth process was conducted 100-200 hours at a fixed temperature and Ar pressure. The grown crystals (Fig. 7) were 60 mm (ZnTe) and 100 mm (CdTe) diameter and 12-15 mm thickness. The dislocation densities of ZnTe and CdTe crystals determining by the chemical etching procedure [25] varied within $(0.8\div3)\times10^4$ cm^{-2} depending on the crystal part. The crystals were free from microprecipitates according to SEM and IR microscopy.

To analyze crystal's nonstoichiometry, we cut samples from different parts of the crystals, (see Fig. 7 bottom), powdered them to 20-40 μm and characterized, as described in Part. 2.1. Besides determination of non-stoichiometry (Table 4) impurity concentrations were measured by the ICP-MS technique (Fig.8).

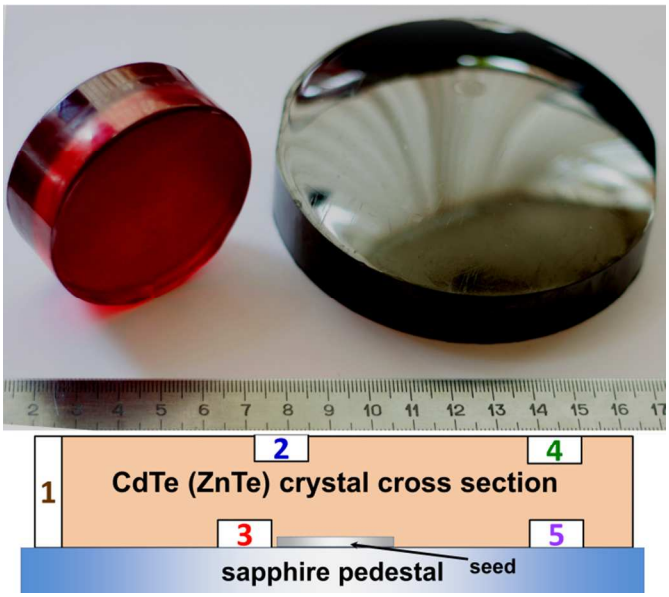

Fig. 7 Images of ZnTe (upper left), CdTe (upper right) crystals grown by Markov-Davydov technique and the scheme of middle cross-section crystal analysis (bottom): the numbers corresponds to the samples in Table 4 and Fig.8

The nonstoichiometry of the vapor-grown ZnTe crystal was in 2-3 times higher than that of CdTe. Te-excess appeared in all parts of the crystal, and the nonstoichiometry was nearly

uniform in the crystal (ZnTe-2, ZnTe-4, ZnTe-5). The lowest nonstoichiometry level was detected close to the seed area (ZnTe-3).

In the CdTe case the major crystal part contained Te-excess. The nonstoichiometry level corresponded to S_{AB}=V conditions on p_{Te2}-T-x diagram (Fig. 6 left). The nonstoichiometry was varying during slow cooling according to the S=V line, and the δ=0 line was crossed. An inversion of the deviation from stoichiometry took place, and Cd-excess in the upper peripheral part of the crystal (CdTe-4) was detected. We attribute it to a more intensive cooling of this crystal part, and S_{CdTe}V equilibrium could be reached more efficiently in this local area. Moreover, this area contained lower level of impurities (Fig.8b).

Table 4. Nonstoichiometry of CdTe and ZnTe vapor grown crystals

N	$m_{Cd(Zn)Te}$, g	$m_{Cd_{extr.}}\times10^6$ g	$m_{Te_{extr.}}\times10^6$ g	$X_{Te(Cd)}$ (mole excess Te(-Cd)/mole CdTe)
		CdTe		
1	0.8661	0.89±0.02	3.84±0.06	$(6.15\pm0.08)\times10^{-6}$
2	0.7191	1.87±0.03	3.70±0.05	$(4.13\pm0.04)\times10^{-6}$
3	0.5758	5.59±0.12	8.22±0.23	$(6.12\pm0.31)\times10^{-6}$
4	0.8385	6.10±0.09	5.69±0.10	$-(2.77\pm0.01)\times10^{-6}$
5	0.7085	5.06±0.08	7.25±0.01	$(4.00\pm0.21)\times10^{-6}$
		ZnTe		
2	0.5657	0.97±0.02	7.80±0.11	$(2.23\pm0.03)\times10^{-5}$
3	0.6152	1.39±0.04	4.87±0.10	$(1.01\pm0.02)\times10^{-5}$
4	0.6924	0.59±0.01	7.03±0.18	$(1.73\pm0.05)\times10^{-5}$
5	0.5852	0.91±0.27	8.09±0.03	$(2.27\pm0.09)\times10^{-5}$

''–'' indicates on Cd excess in CdTe crystal

Due to ICP-MS analysis, impurities were concentrated in the upper central part (CdTe-2, ZnTe-2) while the purity of the peripheral areas was better. On closer examination purity of the CdTe crystal was higher in the bottom peripheral area (CdTe-5), whereas ZnTe crystal contained fewer impurities in the upper peripheral part (ZnTe-4).

For the tested crystals comparison of nonstoichiometry and total impurities concentration showed that for all specimens the impurity content was higher than the excess component concentration. In ZnTe case the ratio ($X_{impurity}/X_{nonstoich}$) varied within 1.5÷2 and for CdTe it was 3÷5. At the measured crystal's resistivity $>10^9$ Om.cm it means that in the case of CdTe and ZnTe crystals grown from vapor by the Markov-Davydov technique the crystal purity is more important characteristic than nonstoichiometry contrary to the melt grown crystals [25].

Conclusions

It was found by direct physico-chemical measurements that the homogeneity regions of undoped ZnTe and CdTe include stoichiometric composition in the 750-1365 K temperature range. The analysis of solidus lines on the studied T–x diagrams combined with XRD measurements let us propose the scheme of wurtzite-sphalerite (3C-2H) polymorphous transition for ZnTe. According to the scheme, the polymorphous transition is followed by peritectic reactions at both Te-rich and Zn-rich sides. In the case of CdTe the solidus line near the melting point demonstrated anomalous behavior which could be explained in terms of high-temperature polymorphous transition but we failed the fixed this polymorph.

Undoped ZnTe (∅60 mm) and CdTe (∅100 mm) single crystals grown by Markov-Davydov technique at 1170-1320 K close to congruent sublimation conditions have a uniform distribution of deviations from stoichiometry $(4\div6)\times10^{-6}$ and $(1\div2)\times10^{-5}$ mole excess Te per mole CdTe or ZnTe, correspondingly. Impurities localized in the central bottom part of grown crystals and their concentrations were less than in the seeds.

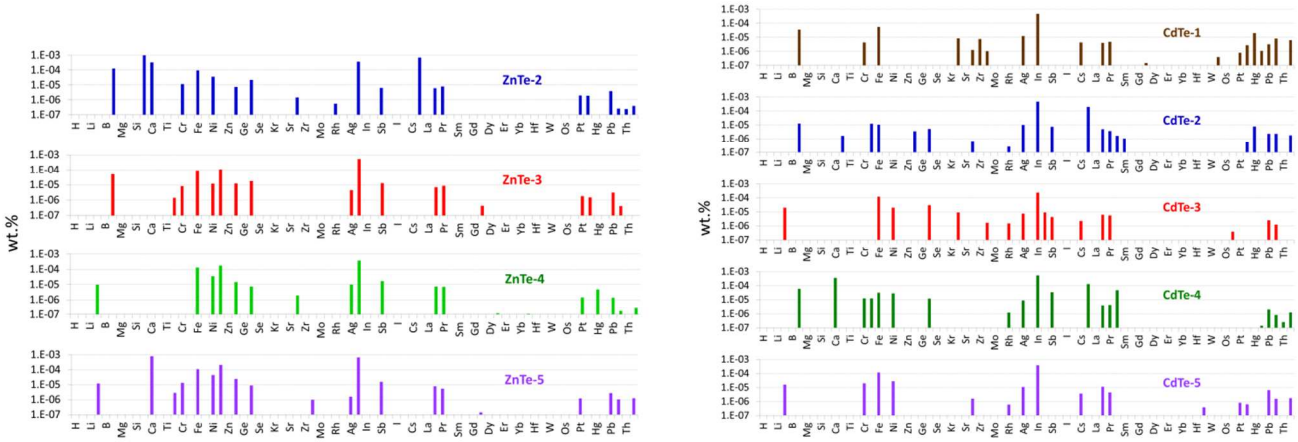

Fig. 8 Impurity distributions in ZnTe (left) and CdTe (right) vapor grown crystals. The crystal's legends correspond to the cross-section on Fig.7.

Acknowledgements

The research was supported by grant U.M.N.I.K. contract 201GU1/2013. Authors also acknowledge D. Mendeleyev Common Use Center for analytical instrument measurements and ARMOLED Ltd. for the technical support.

Notes and references

1 T. Takahashi, S. Watanabe Recent Progress in CdTe and CdZnTe detectors, *IEEE Trans. Nucl. Sci.* 2001,**48**(4), 950.
2 K. Sato, M. Hanafusa, A. Noda, A. Arakawa, M. Uchida, T. Asahi and O. Oda, *J. Cryst. Growth*, 2000, **214-215**, 1080.
3 K. Sato, Y. Seki, Y. Matsuda and O. Oda, , *J. Cryst. Growth,* 1999, **197**(3), 413.
4 R. Triboulet, P. Shiffert CdTe and Related Compounds; Physics, Defects, Hetero- and Nano-structures. Oxford OX2 8DP.: Elsevier Science, 2009
5 Springer Handbook of Electronic and Photonic Materials /Kasp S., Capper P. (Edt.) NY: Springer Science+Business Media Inc. 2007 [P.325-342} Part B. Growth and characterization. 16 Wide-bandgap II-VI Semoconductors. Growth and properties.
6 U. Roy, S. Weiler and J. Stein, *J. Cryst. Growth,* 2010, **312**(19) 2840–2845
7 A. Davydov, E. V. Markov, V. T. Khryapov, *Izvestia AN SSSR Neorg. Mater*, 1992, **16** (12) 2119 (*in Russian)*
8 F. A. Kroeger The Chemistry of Imperfect Crystals , North Holland, Amsterdam, 1964
9 I. Avetissov, E. Mozhevitina, A Khomyakov, T. Khanh *Cryst. Res. Technol.,* 2014, DOI 10.1002/crat.201400201
10 F. T. J. Smith, *J. Phys. Chem. Solids*, 1971, **32**, 2201.
11 T. Feltgen, J. H. Greenberg, A. N. Guskov, M. Fiederle and K. W. Benz, *International Journal of Inorganic Materials,* 2001, **3**, 1241.
12 E. N. Gesko, I. Ch. Avetissov, Ya. L. Kharif ZnTe homogeneity limits. Abstracts of 3rd All-Union conference "Material Science of chalcogenate semiconductors", Chernovtzy, 1991, p.54 (*in Russian*)
13 Spinulescu-Carnaru, *Phys. Status Solidi,* 1966, **18**, 769
14 C. Yeh, Z. W. Lu, S. Froyen and A. Zunger, *Phys. Rev. B,* 1992, **46**, 10086
15 L. B. Pankratz, E. G. King, *U. S. Bur. Mines, Rept. Invest.,* 1965, No.6708, p.1-8
16 M. P. Kulakov, I. V. Balyakina, *J. Cryst. Growth*, 1991, **113**, 653.
17 SGTE (2011) Alloy Database http://www.crct.polymtl.ca/fact /documentation/FSData.htm#SGTE
18 S. A. Medvedev, S. N. Maximovskii, K. V. Kiseleva, et al., *Izvestia AN SSSR Neorgan. Materials.* 1973, **9 (3)**, 356 (*in Russian)*
19 H. Greenberg, V. N. Guskov, V. B. Lazarev and O. V. Shebershneva, *Mater. Res. Bull.* 1992, **27**, 847.
20 Yu. M. Ivanov, *J. Cryst. Growth* 1996, **161**, 12
21 Jouglar, C. Hitroit, P. L. Vuillermoz and R. Triboulet, *J. Appl. Phys.,* 1980, **51**, 3171
22 N. K. Kurbakova. Dependance between synthesis conditions, nonstoichiometry and properties of semiconducting cadmium telluride. Ph.D Thesis, Moscow, 1992 145 p (*in Russian*).
23 Kharif Ya.L., Kovtunenko P.V., Mayer A.A. Thermodynamics of nonschiometric lead and cadmium chalcogenides. in V.M.Glazov and A.V.Novoselova (Eds.) Thermodynamics and Material Science of Semiconductors, Metallurgiya, Moscow, 1992, pp. 247-272 (*in Russian*).
24 I.Ch. Avetissov n, E.A. Sukhanova, A.V. Khomyakov, A.Yu. Zinovjev, V.A. Kostikov and E.V. Zharikov, *J. Cryst. Growth,* 2011, **318**, 528
25 P. Rudolph, N. Schtifer, T. Fukuda, Materials Science and Engineering, 1995, **R15,** 85-133
26 Kh. Avetisov, Yu. M. Ivanov and A. V. Zorin, *J. of Surface Investigation. X-ray, Synchrotron and Neutron Techniques (Poverkhnost'. Rentgenovskie, Sinkhrotronnye i Neitronnye Issledovaniya)* 2001, **10**, 82 (*in Russian*).
27 E. N. Mozhevitina, B. N. Levonovich and I. Ch. Avetisov, *Inorganic Materials,* 2013, **49**, 439
28 I.Ch.Avetisov, E.N.Mozhevitina, A.V.Khomyakov, R.I.Avetisov, A.Yu.Zinovjev, *Izvestuia VUSov Materiali elektronnoi tekhniki*, 2013, **1**, 4-10
29 H.R. Vydyanath, J. Ellsworth, J.J. Kennedy, B. Dean, C.J. Johnson, G.T. Neugebauer, J. Sepich, P.K. Liao, *J. Vac. Sci. Technol. B* 1992 10(4), 1476

[a] Address, Miusskaya pl. 9, Moscow, 125047, Russia. Fax: 7-495-496-6781; Tel: 7-495-496-6177; E-mail: aich@rctu.ru.
[b] Address, Proezd 4806, 4-2, Zelenograd, Moscow, 124460, Russia. Fax: 7-499-720-8364; Tel: 7-499-731-1476; E-mail: info@niimv.ru.

Homogeneity limits and nonstoichiometry of vapor grown ZnTe and CdTe crystals

I. Ch. Avetissov, E. N. Mozhevitina, A. V. Khomyakov, R. I. Avetisov, A. A. Davydov, V. P. Chegnov, O. I. Chegnova and N. V. Zhavoronkov

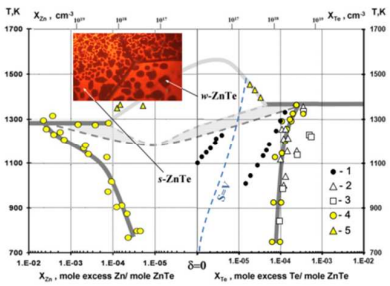

A new understanding of wurtzite-spalerite phase transition in CdTe and ZnTe compounds in connection with vapor growth of single crystals